Competition constrains parasite adaptation to thermal heterogeneity

Samuel TE Greenrod[1#], Daniel Cazares[1], Weronika Slesak[1], Tobias E Hector[1], R. Craig MacLean[1,2], Kayla C King[1,3,4,#]

[1] Department of Biology, University of Oxford, Oxford, UK

[2] All Souls College, High Street, Oxford OX1 4AL, UK

[3] Department of Zoology, University of British Columbia, Vancouver, Canada

[4] Department of Microbiology & Immunology, University of British Columbia, Vancouver, Canada

[#]Correspondence: greenrodsam@gmail.com (Samuel Greenrod); kayla.king@ubc.ca (Kayla King)

Abstract

Temporal thermal heterogeneity is expected to favour intermediate, generalist phenotypes that can maintain growth across a broad thermal range but have sub-optimal growth at any single temperature. Yet, thermal variation typically occurs in the presence of additional selection pressures which may interact to constrain adaptation to temperature. We propagated competing lytic viral parasites (bacteriophages ϕ14-1 and ϕLUZ19) of *Pseudomonas aeruginosa* under fluctuating temperatures (37-42°C) in monoculture and in co-culture. Without competition, fluctuating temperatures favoured intermediate thermal phenotypes in the phage ϕ14-1 and resulted in more variable evolutionary outcomes compared to static conditions. However, co-selection from fluctuating temperatures and competition led to restricted thermal adaptation, slower evolutionary rates, and fewer putative adaptive mutations in the ϕLUZ19 competitor. Our study highlights the potential for reduced adaptive capacity in interacting communities amidst global climate change.

Introduction

Thermal heterogeneity plays a key role in shaping species' evolutionary trajectories. Spanning a broad range of timescales, temperatures fluctuate across multi-year periods (ENSO), between seasons, and even on the order of hours through diurnal (24-hour) cycles. Very slow or rapid thermal fluctuations typically lead to similar adaptation to static environments through selective sweeps by specialist variants [1,2]. Moderate fluctuations select for thermal generalists which have intermediate phenotypes across temperatures [1,2]. Generalist phenotypes often arise through the acquisition of multiple specialist mutations [3] or single pleiotropic mutations [4]. Thermal heterogeneity can also promote diversifying selection [5–7] leading to the maintenance of thermal specialist sub-populations [6]. The mechanisms of adaptation to thermal heterogeneity depend on the fluctuation frequency relative to generation time [8]; fluctuations that favour specialists in fast-replicating species may select for generalists in slow-replicating species.

Thermal heterogeneity typically occurs in the context of multiple selective pressures. For example, warming can impose selection on species that are simultaneously adapting to other

abiotic stressors or to interactions with predators, competitors, or antagonists [9,10]. The presence of multiple selection pressures can constrain evolution rates through combined negative effects on species fitness which reduce population sizes and mutational supply [11,12]. Co-selection can also restrict adaptation through pleiotropic fitness trade-offs; high fitness under one stressor reduces fitness under another [13,14]. Spatial thermal heterogeneity is expected to promote genetic diversification by increasing niche differences [15]. Similar findings have been shown with regards to temporal heterogeneity [16]. Thermal fluctuations may offset the diversity-suppressing impacts of co-selection. However, some studies have indicated that co-selection involving temporal heterogeneity can exacerbate evolutionary constraint [17–19]. The ability of species to adapt to thermal heterogeneity amidst other selection pressures plays an important role in the maintenance of global biodiversity and species extinction risk [11,20–22].

Parasites, across the tree of life, provide an ideal group of organisms to study adaptation to thermal heterogeneity. Parasites are often exposed to diverse environments and stressors across their multi-stage life cycles. They can have both free-living, vector-based, and host-associated life stages [23]. By moving through numerous external environments during and between replicative cycles, parasites experience high temporal thermal heterogeneity (Greenrod et al., in press; [24]). During the infection stage, parasites can also induce fevers in hosts, driving thermal changes [25]. Finally, parasites are expected to face increasingly frequent thermal extremes as a result of global climate change [26]. While contending with variable thermal environments, parasites must adapt to host immune responses [27] and competition with co-infecting parasites in the same host population or individual [28]. Within and between-host competition are primary determinants of parasite virulence [29] signifying that interactions between competition and environment-based selection can shape parasite evolution [30].

We predicted that thermal heterogeneity would select for generalist parasite populations, which have intermediate phenotypes, and promote genetic diversity [1]. We also predicted that co-selection with other environmental stressors would constrain parasite adaptation [17]. We passaged two lytic viral parasites (thermal generalist ϕLUZ19 and specialist ϕ14-1) under a fluctuating thermal regime (37-42°C) in the absence and presence of a phage competitor. Phages evolved with a static bacterial host, *Pseudomonas aeruginosa*. We compared populations evolved under fluctuating temperatures concurrently with those evolved under a static regime (37°C and 42°C), the latter presented in ref. [31]. We evaluated phage phenotypic adaptation through growth assays at 37°C and 42°C. We also conducted phage population sequencing to identify adaptive mutations and measure evolutionary rates.

Methods and Materials

Strains, Storage, and Culture Conditions

This study builds on a previously published experimental framework [31] using the same bacterial host and bacteriophage strains. *Pseudomonas aeruginosa* PAO1 was used as the non-evolving bacterial host throughout. Two lytic phages, ϕLUZ19 and ϕ14-1, were used due

to their known thermal response differences: ϕLUZ19 performs well at both 37°C and 42°C, while ϕ14-1 is growth-restricted at 42°C [31,32]. Phage lysates and bacterial stocks were prepared as in refs [31,32].

Experimental Evolution

The experimental evolution design closely followed that of ref. [31] with additional treatments incorporating fluctuating temperatures. Phages were serially passaged for 15 days under four conditions: monoculture and co-culture, each at either static or fluctuating temperatures (daily shifts between 37°C and 42°C). Each treatment included six independent replicate populations initiated from a single ancestral lysate.

Phages were propagated without shaking with a non-evolving ancestral PAO1 bacterial host. For the initial passage, ancestral phage lysates were diluted to 10^8 PFU/ml and 300µl were added to 2.7ml 10^8 CFU/ml bacterial culture in loose-lid 14ml falcon tubes. Phage co-culture lines were prepared by combining 150µl each of ϕLUZ19 and ϕ14-1 10^8 PFU/ml lysates prior to mixing with bacteria. The initial passage phage densities were ~10^7 PFU/ml resulting in a phage/bacteria ratio (multiplicity of infection, MOI) = ~0.1. Following addition of bacterial cultures, tubes were incubated statically at 37°C or 42°C in circulating water baths for 8h. Fluctuating passages started and ended at 37°C.

After incubation, phage populations were harvested by centrifugation (3,095×g, 5 min) to pellet bacteria, followed by sterile filtration through 0.2µm filters. Filtrates were stored at 4°C. In subsequent passages, 300µl of lysate was transferred into fresh PAO1 cultures.

Phage Quantification

Phage titres were determined via the double-layer overlay method [33] following the same protocols as in refs [31,32]. Briefly, bacterial lawns were prepared by mixing 10mL of melted LB-top agar with 300µL of a *P. aeruginosa* PAO1 overnight culture. Phage lysates were serially diluted, and 10µL was spotted onto the bacterial lawns. After incubating plates for 6–8 h at 37°C, spots with the highest number of discernible plaques were counted and reported. ϕLUZ19- or ϕ14-1-resistant PAO1 strains were used for selective plating enabling separate counting of ϕLUZ19 and ϕ14-1 densities in co-cultures. These resistant strains were derived by isolating colonies growing on high titre phage plaques and confirmed via sequencing [31]. All monoculture and co-culture samples were quantified using the appropriate resistant strains to ensure consistency.

Phage Separation and Concentration

To generate high-titre and pure phage lysates for downstream assays and sequencing, we employed selective double-layer overlays with resistant hosts. Briefly, phages and ϕLUZ19- or ϕ14-1-resistant PAO1 strains were seeded into top agar plates to allow phage propagation. Phages were extracted from plates by scraping top-agar into 15ml falcon tubes containing 5ml of phage buffer (NaCl (100 mM), $MgSO_4$ (10 mM), $CaCl_2$ (5 mM), Tris-HCl (pH 8) (50 mM), Gelatin (0.01%)). Tubes were mixed overnight after which phages were separated from top agar using sterile-filtration. This process was performed three times to ensure removal of

phage competitors from co-culture populations. The purification and extraction protocols were identical to those described in ref. [31].

Fitness Assays

Growth Rates

The fitness of purified evolved phage lines relative to the ancestor was assessed by measuring phage and bacterial growth across an 8h window under static incubation at 37°C and 42°C. Phage lysates were diluted to 10^5 PFU/ml and 300uL was mixed with 2.7ml of 10^8 CFU/ml wild-type PAO1 to a final MOI = ~0.0001. ϕLUZ19 was sampled at 2h, 4h, and 8h; ϕ14-1 at 4h and 8h due to delayed replication. Phage quantification was performed through sterile-filtration through 0.22µm filter plates (Agilent) followed by centrifugation at 2,230xg for 5 mins before spotting onto resistant PAO1 double-layer overlay plates. Each growth rate assay included a single replicate of each evolved phage line and three replicates of the phage ancestor. Growth rate assays were repeated three times across a two-week period to produce three technical replicates.

Phage Population Genomics

DNA Extraction and Sequencing

Phage DNA was extracted from purified lysates as described in [31]. Briefly, ancestral and evolved phage lysates were treated with DNase and RNase to remove bacterial DNA and RNA. Phage particles were lysed using lysis (AL) buffer and proteinase K. Cell debris was precipitated using precipitation (N4) buffer and removed. Finally, DNA was precipitated and washed using isopropanol and ethanol. DNA quality was assessed with NanoDrop 2000c (Thermo Scientific) and quantified with Qubit 4 (Thermofisher). Short-read Illumina sequencing was performed by AZENTA/GENEWIZ using their Microbe-EZ pipeline for evolved and ancestral lines. Bacterial genomes (wild-type and phage-resistant strains) were sequenced by MicrobesNG using long-read approaches.

Sequence Analysis

Phage reads were pre-processed with Trim Galore (v.0.5.0) (https://github.com/FelixKrueger/TrimGalore) and downsampled using bbnorm from the bbmap package (v.39.18) (https://sourceforge.net/projects/bbmap/). Reads were then mapped to de novo ancestral assemblies generated with shovill (v1.1.0) (https://github.com/tseemann/shovill) using Bowtie2 (v.2.3.4.2) [34]. Variants were identified using breseq (v.0.36.1) [35]. Ancestral assemblies were annotated with prokka (v.1.14.5) [36], guided by the NCBI GenBank file for each phage (ϕ14-1: NC_011703; ϕLUZ19: NC_010326).

Wild-type and resistant PAO1 genomes were assembled using Autocycler (v. 0.4.0) [37] and polished via Polypolish (v. 0.6.0) [38]. Final assemblies were re-oriented with Dnaapler (v. 1.2.0) [39] and annotated using prokka (v.1.14.5) [36]. The workflow was deployed using a Dockerised Nextflow pipeline (v. 1.0.2) available at https://doi.org/10.5281/zenodo.15706447. Mutations in resistant PAO1 strains were

identified by mapping long reads to the wild-type assembly with minimap2 (v.2.24) [40] and variant calling with medaka (v.2.1) (https://github.com/nanoporetech/medaka). All bioinformatic analyses were conducted with default parameters.

Statistical Analyses and Visualisation

All statistical analyses and data visualisation were conducted using packages in R (v.4.3.2) and RStudio [41,42]. Data wrangling was performed using "Tidyverse" (v.2.0.0) R packages [43]. Phage growth and evolution rates were compared between evolution treatments using linear mixed effect models with the "lme4" (v.1.1-36) R package [44] where the response variable was phage density (pfu/ml) or genetic distance from ancestor, the explanatory variables were an interaction term between evolution treatment and temperature, and batch was a random effect. Within-group variation in genetic distance from ancestor was analysed using Levene's test. The prevalence of unique compared to shared mutations across evolution treatments was analysed using Fisher's exact test. Phage genetic distance between groups was also compared by constructing neighbour-joining trees based on Euclidean genetic distance using the "ggtree" (v.3.10.1) R package [45]. Data and code used in analyses can be found at https://github.com/SamuelGreenrod/Evol_fluctuating.

Results

Fluctuating temperatures select for generalist phenotypes in monoculture

Fluctuating environments can favour generalists with intermediate phenotypes across conditions [1]. Given ϕ14-1 has previously been shown to grow poorly at 42°C, we hypothesised that ϕ14-1 populations passaged under fluctuating conditions would rapidly adapt to 42°C but have lower fitness at 37°C and 42°C compared to static evolved populations. In monoculture, ϕ14-1 grew during 37°C passages but showed little growth in 42°C passages (Fig. 1A). ϕLUZ19 monoculture populations reached and then maintained high densities in all passages. This phage showed low variation in inter-passage densities.

We assessed phage evolution by measuring the growth rates of static and fluctuating evolved lines relative to the ancestral phage through growth assays at 37°C and 42°C (Fig. 1B). We found that growth rates of both phages in monoculture depended on the interaction between evolution treatment and assay temperature (ϕ14-1: $F_{3,29} = 125.8$, $p < 0.001$; ϕLUZ19: $F_{3,29} = 96.0$, $p < 0.001$). At 42°C, ϕ14-1 fluctuating populations were found to have an intermediate phenotype between those evolved under static conditions. ϕ14-1 fluctuating populations had significantly higher growth rates at 42°C than 37°C static populations ($t(29) = -12.4$, $p < 0.001$) but lower growth rates than 42°C static populations ($t(29) = 12.7$, $p < 0.001$). At 37°C, ϕ14-1 fluctuating lines had no significant difference to static populations possibly due to phage growth being measured after phages had reached carrying capacity (see ref. [31]). For ϕLUZ19, fluctuating evolved populations had significantly higher growth at 42°C than 37°C static populations ($t(29) = -19.3$, $p < 0.001$). However, growth was not significantly different to 42°C evolved populations ($t(29) = -1.65$, $p = 0.37$). The opposite findings were observed at

37°C; fluctuating evolved populations had significantly higher growth rates than those evolved at 42°C but similar growth rates to 37°C evolved populations (42°C static: $t(29) = -5.2$, $p < 0.001$; 37°C static: $t(29) = -0.99$, $p = 0.75$).

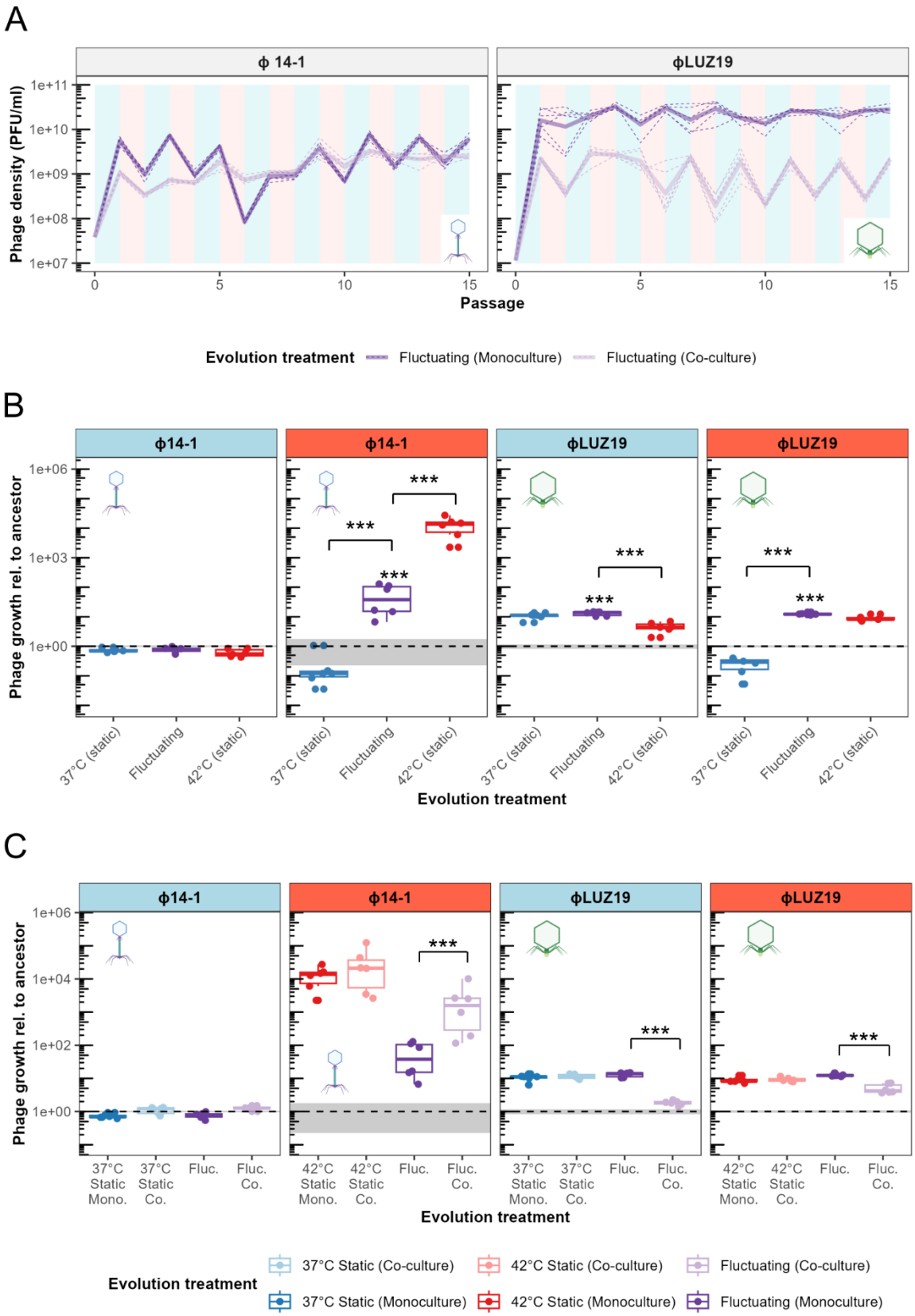

Figure 1. Co-selection in communities constrains adaptation to thermal fluctuations. A) Population dynamics of phages passaged in monoculture and co-culture under fluctuating temperatures. Values show densities at the end of each passage prior to dilution. Plot background colour reflects the temperature during that passage where light blue is 37°C and light red is 42°C. Phage icons illustrate the two different phages used in the experiments (ϕ14-1, myovirus in blue; ϕLUZ19, autographivirus in green) [46] and are used hereafter to refer to phages in figures. **B**) Fluctuating and static temperature evolved population growth rates relative to the ancestor. Growth rates were measured after 2h for ϕLUZ19 and 4h for ϕ14-1. Six biological replicates were assayed, and data points show the average of three technical replicates. Panel strip colour reflects the temperature that growth was tested at where light blue is 37°C and light red is 42°C. Fluctuating populations are presented in purple with 37°C static populations in blue and 42°C static populations in red. Ancestral growth is shown by dashed grey line with standard errors shown as a grey box (n = 3). *** = $p < 0.001$. Absence of asterisk reflects non-significance. Static monoculture temperature data was adapted from ref. [31]. **C**) Growth rates of fluctuating and static temperature monoculture evolved populations compared to co-culture evolved populations. Boxes are coloured by evolution treatment with monoculture in dark (37°C static in blue, 42°C static in red, and fluctuating in purple) and co-culture in light (37°C static in light blue, 42°C static in light red, and fluctuating in light purple). Assay temperature and significance values are presented as in Fig. 1B. Six biological replicates were assayed and data points show the average of three technical replicates. Ancestral growth rates and significance signs are presented as in Fig. 1B. Static co-culture data was adapted from ref. [31].

Co-selection from fluctuating temperatures and competition constrains thermal adaptation

The presence of additional selection pressures is expected to constrain adaptation to fluctuating temperatures by reducing mutational supply and compounding fitness trade-offs [11,18,19]. We hypothesised that phages evolved under co-selection from fluctuating temperatures and competition would have lower fitness at 37°C and 42°C than those evolved under static temperatures or fluctuating monoculture conditions. While ϕ14-1 densities fluctuated between passages in monoculture, co-culture densities rapidly increased and then stabilised between passages (Fig. 1A). In contrast, ϕLUZ19 populations were stable in monoculture, but during fluctuations in co-culture, experienced high growth at 37°C and low growth at 42°C.

We then assessed evolved phage growth rates at 37°C and 42°C (Fig. 1C). We found a significant interaction between evolution treatment (monoculture and co-culture) and temperature regarding growth rates for both phages (ϕ14-1: $F_{6,59} = 75.0$, $p < 0.0001$; ϕLUZ19: $F_{6,59} = 103.5$, $p < 0.0001$). While competition had no impact on the growth rates of static ϕ14-1 populations (37°C: $t(59) = -0.78$, $p = 0.99$; 42°C: $t(59) = -0.98$, $p = 0.99$), fluctuating co-culture evolved populations had significantly higher growth rates at 42°C compared to populations evolved in monoculture ($t(59) = -6.7$, $p < 0.0001$). No significant difference was observed at 37°C ($t(59) = -1.0$, $p = 0.99$). Similar to ϕ14-1, there was no impact of competition on static evolved ϕLUZ19 population growth rates (37°C: $t(59) = -0.42$, $p = 1.0$; 42°C: $t(59) = -0.21$, $p = 1.0$). However, ϕLUZ19 populations evolved with fluctuations and competition had

significantly lower growth rates at both 37°C and 42°C compared to monoculture (37°C: $t(59) = 10.1$, $p < 0.0001$; 42°C: $t(59) = 4.9$, $p < 0.001$).

Fluctuating environments favour specialist mutations

Fluctuating temperatures generally select for multiple specialist mutations [3]. We hypothesised that fluctuating evolved populations would show genetic similarities to both high and low temperature static lines. Phage genomic evolution was assessed by constructing neighbour-joining trees based on Euclidean genetic distances (Fig. 2A). Fluctuating evolved populations did not form a unique clade but instead were found to co-locate with either high or low temperature static populations. ϕ14-1 fluctuating populations were distributed across the tree and generally did not cluster with static populations. Conversely, ϕLUZ19 fluctuating populations were primarily found within the 42°C static clade.

We further analysed static and fluctuating population genetic similarities by measuring evolution rates based on Euclidean genetic distance from ancestor (Fig. 2B). For ϕ14-1, fluctuating evolved populations had significantly lower evolution rates than 42°C static populations ($t(15) = -4.1$, $p < 0.01$). However, evolution rates were equal between fluctuating and 37°C static populations ($t(15) = -0.51$, $p = 0.87$). There was no significant difference in evolution rates between ϕLUZ19 fluctuating populations and either 37°C or 42°C static populations (37°C: $t(15) = -0.46$, $p = 0.89$; 42°C: $t(15) = -0.75$, $p = 0.74$). Notably, ϕ14-1 fluctuating populations had significantly greater within-group variation in evolution rates compared to 42°C static populations ($t(15) = 2.9$, $p < 0.05$) but not 37°C static populations ($t(15) = -0.70$, $p = 0.77$). ϕLUZ19 fluctuating populations had no significant difference in within-group variation compared to static populations (37°C: $t(15) = 2.0$, $p = 0.15$; 42°C: $t(15) = -0.10$, $p = 0.99$).

We then determined the prevalence of high frequency genetic variants (> 20% frequency) that were unique to or shared between evolution treatments (Fig. 2C). For ϕ14-1, 2/11 (18%) of 37°C static variants and 5/15 (33%) of 42°C static variants were shared with other evolution treatments compared to 4/9 (44%) variants in fluctuating evolved populations. For ϕLUZ19, shared variants constituted 8/32 (35%) of 37°C static and 9/20 (45%) of 42°C static variants compared to 12/17 (71%) in fluctuating evolved populations. Despite the trend for more shared mutations in fluctuating evolved populations, there was no significant difference in the prevalence of shared mutations relative to unique mutations between evolution treatments for ϕ14-1 or ϕLUZ19 (Fisher's exact test: ϕ14-1, $p = 0.47$; ϕLUZ19, $p = 0.08$).

Finally, we investigated which mutations drove clustering between fluctuating and static populations (Fig. S1; Table S1). While ϕ14-1 fluctuating and 37°C static populations showed little clustering, two fluctuating populations clustered with the 42°C static clade. These two replicate populations contained parallel deletions in a hypothetical protein with high similarity to a DNA ligase (BlastP: 97.47% identity, 95% sequence overlap with Pseudomonas phage PhL_UNISO_PA-DSM_ph0031 DNA ligase protein), previously identified in all ϕ14-1 42°C static populations [31]. The clustering of 5/6 ϕLUZ19 fluctuating populations with the 42°C static populations were attributed to parallel insertions in an intergenic region between

two hypothetical proteins. This intergenic insertion was also previously identified in all ϕLUZ19 42°C static populations [31].

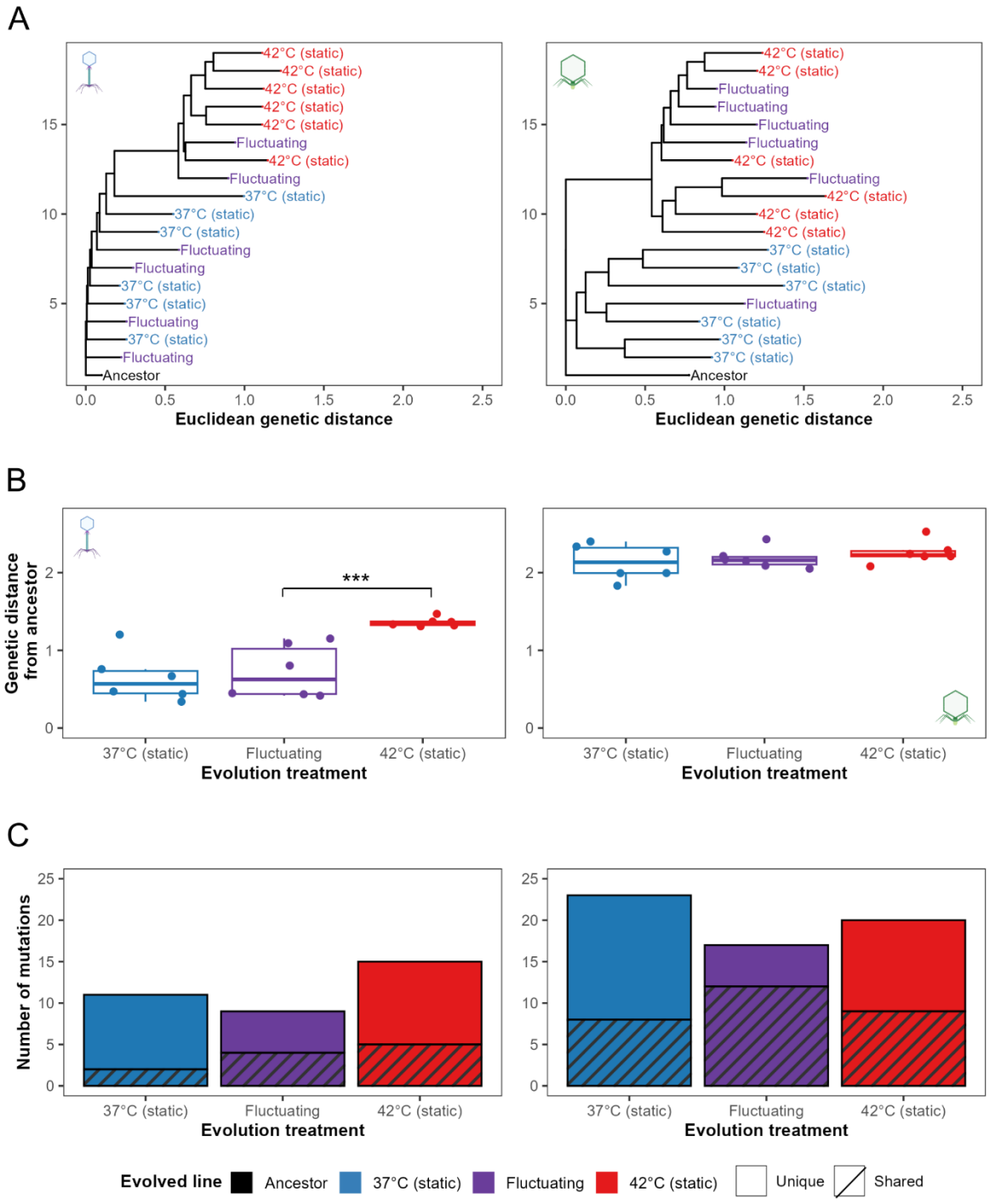

Figure 2. Fluctuating temperatures select for specialist mutations. A) Neighbour-joining trees of evolved and ancestral phage populations constructed using Euclidean genetic distances. Genetic distances were calculated based on the presence and frequency of mutations present at > 10% frequency. Tree is rooted at the ancestor and populations are coloured by evolved treatment. **B**) Phage evolution rates, measured based on Euclidean

genetic distance from the ancestor, for evolved monoculture phage populations. *** = $p < 0.001$. **C**) Stacked bar charts show the number of high frequency variants (> 20% frequency) that are unique to or shared between evolution treatments. Bars are coloured by evolution treatment. Unique genes are shown as clear bars and shared genes are shown as striped bars. Static temperature data was adapted from ref. [31].

Co-selection constrains molecular evolution

By reducing growth rates, co-selection from fluctuating temperatures and competition are expected to reduce evolution rates and restrict the acquisition of adaptive mutations [11]. Due to their elevated growth rates, we hypothesised that ϕ14-1 fluctuating co-culture populations would have higher evolution rates than monoculture populations. No significant difference in evolution rate was observed for ϕ14-1 co-culture populations compared to monoculture populations ($F_{1,10} = 4.1$, $p = 0.07$) (Fig. 3A). However, non-significance was driven by a single low evolution rate replicate in the co-culture treatment; when the replicate was removed, co-culture populations had significantly greater evolution rates than monoculture ($F_{1,9} = 8.6$, $p < 0.05$). We also found no significant difference in within-group variation in evolution rates between monoculture and co-culture populations ($t(10) = 1.50$, $p = 0.17$), although the difference was also significant once the low evolution rate co-culture replicate was removed ($t(10) = 3.6$, $p < 0.01$).

For ϕLUZ19, we hypothesised that fluctuating co-culture populations would have lower evolution rates than monoculture populations due to the suppression of ϕLUZ19 by ϕ14-1. ϕLUZ19 fluctuating co-culture populations had significantly lower evolution rates than monoculture populations ($F_{1,10} = 470$, $p < 0.001$). We further hypothesised that ϕLUZ19 fluctuating co-culture populations, but not ϕ14-1 populations, would have lower evolution rates than 37°C or 42°C static co-culture populations. Evolution rates were equal between co-culture populations for ϕ14-1 ($F_{2,15} = 1.2$, $p = 0.3$) (Fig. 3B). However, ϕLUZ19 fluctuating co-culture populations were found to have significantly lower evolution rates than both 37°C static and 42°C static monoculture populations (37°C: $t(15) = 4.5$, $p < 0.01$; 42°C: $t(30) = 3.0$, $p < 0.05$).

Finally, we assessed the impact of competition on the acquisition of high frequency mutations (> 20% frequency) in fluctuating populations (Fig. S2). For ϕ14-1, while populations no longer acquired singleton mutations, all populations acquired a deletion or SNP in a putative DNA ligase gene. Mutations in this gene are thought to contribute to high temperature adaptation [31] and were also found in the two monoculture populations which clustered with 42°C static populations in Fig. 2A. For ϕLUZ19, while co-culture populations maintained mutations in tail fiber genes, the populations no longer acquired singleton mutations or the intergenic insertion associated with 42°C static populations.

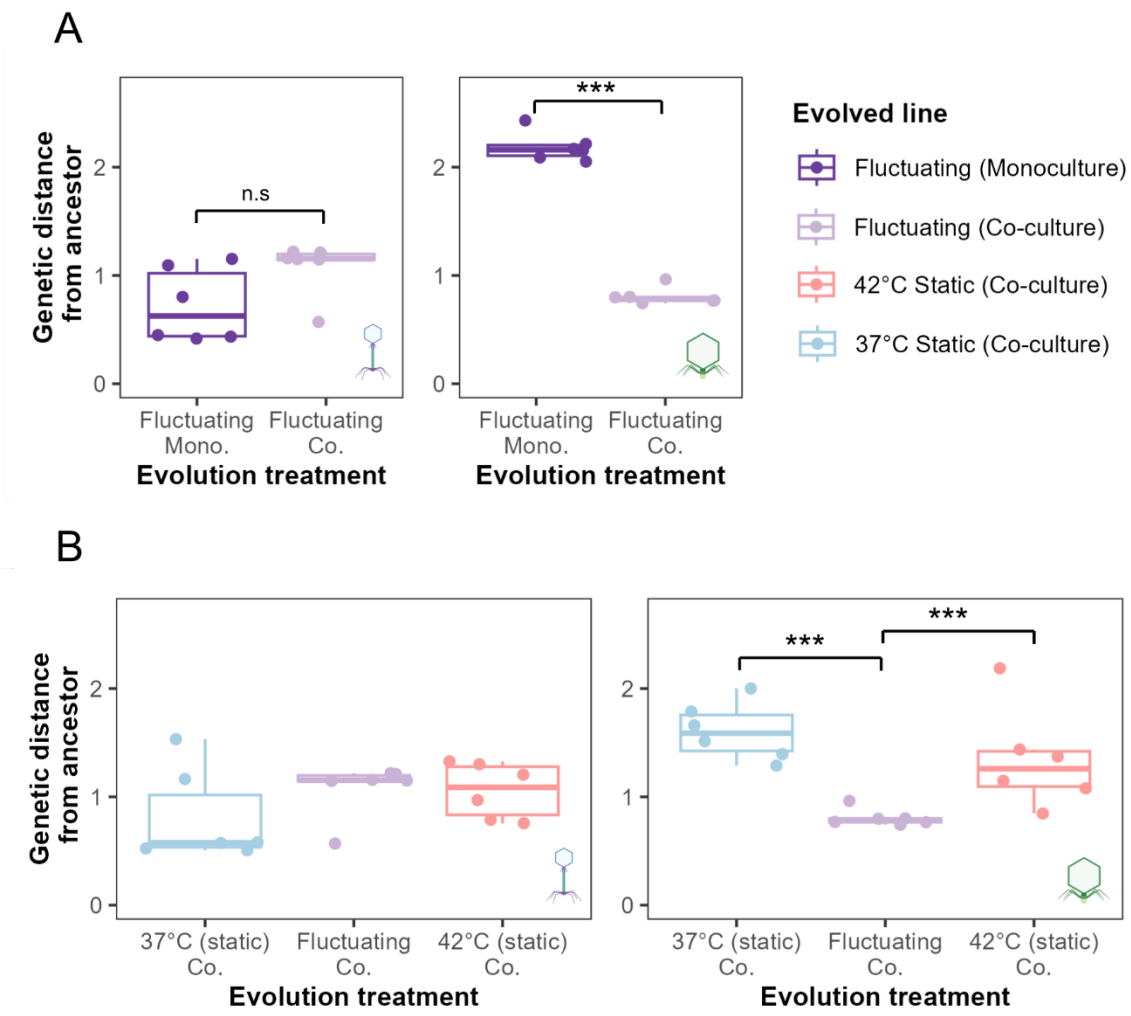

Figure 3. High environmental complexity constrains evolution rates. **A**) Evolution rates, measured based on Euclidean genetic distance from the ancestor, of phage populations evolved under fluctuating temperatures in monoculture (deep purple) and co-culture (light purple). **B**) Evolution rates of 37°C static, fluctuating, and 42°C static co-culture populations. Plot layout is the same as panel A. *** = $p < 0.001$. N.S is used to denote lack of statistical significance. Static temperature data was adapted from ref. [31].

Discussion

Under fluctuating selection, both phages were found to rapidly evolve increased growth rates at high temperatures. For phage ϕ14-1, fluctuating temperatures favoured intermediate thermal phenotypes with lower growth rates at high temperatures compared to phages evolved under static temperatures. The evolution of intermediate phenotypes is likely due to weaker selection for adaptation to high temperatures in the fluctuating treatment. Alternatively, adaptation to high temperatures may be constrained during fluctuations due to fitness trade-offs at lower temperatures [47]. For phage ϕLUZ19, fluctuating temperature populations had the same thermal phenotypes as sympatric static-evolved populations. Given ϕLUZ19 was shown to exhibit fitness trade-offs under static selection [31], this finding is

indicative of a no-cost generalist strategy [48]. The lack of fitness costs may reflect an epistatic pleiotropy, whereby the costs of adaptive mutations depend on the genetic background [48]. Costs may also occur in unmeasured traits such as virulence [49] or tolerance to other stresses [14]. These findings highlight that, while fluctuating temperatures select for greater high temperature growth, the exact phenotypic outcomes of fluctuating selection vary between phage taxa.

We found that fluctuating temperatures resulted in more variable evolutionary trajectories; while static evolved populations generally formed clusters, fluctuating populations were genetically similar to both 37°C and 42°C static evolved populations. Further, we found that parallel mutations acquired under fluctuating selection were the same as those previously identified in static evolved populations [31]. These findings could be explained by historical contingency [50] whereby random mutations that are adaptive at low or high temperatures become fixed in a subset of populations [6]. Depending on the timing of mutation appearance, fluctuating populations may then resemble individual static environments. Fluctuating environments have also been shown to select for mutations conferring fitness in the most extreme environment [51]. The clustering of ϕLUZ19 fluctuating populations with 42°C static populations likely reflects selective sweeps combined with asymmetrical selection where 42°C adaptive variants are fixed more rapidly.

While fluctuating environments can promote genetic diversification, co-selection with other environmental stressors can constrain adaptation [11]. Uiterwaal et al [18] showed that combined fluctuating temperatures and predation restricted adaptation to both selection pressures in *Paramecium caudatum* populations. Similar findings have also been observed in *Daphnia magna* with co-selection from thermal fluctuations and predation/pollutants [19,52]. We found that combined fluctuating temperature- and competition-based selection constrained both thermal adaptation and slowed evolutionary rates in phage ϕLUZ19. Further, co-selection resulted in greater ϕLUZ19 evolutionary constraint with fluctuating temperatures than static temperatures. The negative effects of combined environmental stressors are often non-additive and instead exhibit synergies [11]. We have previously shown that selection from high temperatures synergises with competition to constrain ϕLUZ19 evolution rates [31]. The present study extends these findings by showing that the selective synergy between temperature and competition is greater under fluctuating temperatures than static temperatures. One potential explanation for these findings is that fluctuating environments reduce the strength of selection for adaptive mutations [53]. Weaker directional selection combined with suppression by competitors may constrain both the supply and fixation of beneficial mutations leading to particularly low evolution rates.

Anthropogenic activities, including global climate change, mean that species are facing increasingly variable and complex environments [54]. With ongoing global biodiversity loss, species must adapt to tolerate environmental stressors to avoid extinctions. Our findings highlight that while species can rapidly adapt in response to thermal variation, co-selection with other stressors, such as competition, may restrict species adaptive capacity. These results have particular relevance for parasites which must simultaneously adapt to both thermal heterogeneity, community competition in coinfections, and host immune responses.

With global parasite biodiversity at risk due to climate change [26], evolutionary constraint caused by co-selection may prevent parasite adaptation to thermal stress and further increase the probability of parasite extinctions. Future studies should consider the evolution-constraining effects of co-selection when assessing species extinction risk in thermally variable environments.

Acknowledgments

We thank R. Salguero-Gomez, T. Richards, T. Barraclough, and K. Foster for feedback on the experimental design and results. This work was supported by the Biotechnology and Biosciences Research Council (BB/T008784/1) to S.T.E.G. as well as the Natural Environment Research Council (NE/X000540/1) and NSERC Canada Excellence Research Chair to K.C.K. The funders had no role in study design, data collection and interpretation, or the decision to submit the work for publication. Phage sequence reads are accessible on NCBI (https://www.ncbi.nlm.nih.gov/) under BioProject ID: PRJNA1334331.

References

1. Kassen R. The experimental evolution of specialists, generalists, and the maintenance of diversity. Journal of Evolutionary Biology. 2002;15(2):173–90.

2. Sachdeva V, Husain K, Sheng J, Wang S, Murugan A. Tuning environmental timescales to evolve and maintain generalists. Proceedings of the National Academy of Sciences. 2020 Jun 9;117(23):12693–9.

3. Lambros M, Pechuan-Jorge X, Biro D, Ye K, Bergman A. Emerging Adaptive Strategies Under Temperature Fluctuations in a Laboratory Evolution Experiment of Escherichia Coli. Front Microbiol. 2021 Oct 22;12:724982.

4. Sandberg TE, Lloyd CJ, Palsson BO, Feist AM. Laboratory Evolution to Alternating Substrate Environments Yields Distinct Phenotypic and Genetic Adaptive Strategies. Appl Environ Microbiol. 2017 Jun 16;83(13):e00410-17.

5. Abdul-Rahman F, Tranchina D, Gresham D. Fluctuating Environments Maintain Genetic Diversity through Neutral Fitness Effects and Balancing Selection. Molecular Biology and Evolution. 2021 Oct 1;38(10):4362–75.

6. Harrison E, Laine AL, Hietala M, Brockhurst MA. Rapidly fluctuating environments constrain coevolutionary arms races by impeding selective sweeps. Proc Biol Sci. 2013 Aug 7;280(1764):20130937.

7. Chesson P. Mechanisms of Maintenance of Species Diversity. Annual Review of Ecology, Evolution, and Systematics. 2000 Nov 1;31(Volume 31, 2000):343–66.

8. Gilchrist GW. Specialists and Generalists in Changing Environments. I. Fitness Landscapes of Thermal Sensitivity. The American Naturalist. 1995;146(2):252–70.

9. Gunderson AR, Armstrong EJ, Stillman JH. Multiple Stressors in a Changing World: The Need for an Improved Perspective on Physiological Responses to the Dynamic Marine Environment. Annual Review of Marine Science. 2016 Jan 3;8(Volume 8, 2016):357–78.

10. Hector TE, Hoang KL, Li J, King KC. Symbiosis and host responses to heating. Trends in Ecology & Evolution. 2022 Jul 1;37(7):611–24.

11. Crain CM, Kroeker K, Halpern BS. Interactive and cumulative effects of multiple human stressors in marine systems. Ecology Letters. 2008;11(12):1304–15.

12. Hiltunen T, Cairns J, Frickel J, Jalasvuori M, Laakso J, Kaitala V, et al. Dual-stressor selection alters eco-evolutionary dynamics in experimental communities. Nat Ecol Evol. 2018 Dec;2(12):1974–81.

13. Burmeister AR, Fortier A, Roush C, Lessing AJ, Bender RG, Barahman R, et al. Pleiotropy complicates a trade-off between phage resistance and antibiotic resistance. Proceedings of the National Academy of Sciences. 2020 May 26;117(21):11207–16.

14. Schou MF, Engelbrecht A, Brand Z, Svensson EI, Cloete S, Cornwallis CK. Evolutionary trade-offs between heat and cold tolerance limit responses to fluctuating climates. Science Advances. 2022 May 27;8(21):eabn9580.

15. van Houte S, Padfield D, Gómez P, Luján AM, Brockhurst MA, Paterson S, et al. Compost spatial heterogeneity promotes evolutionary diversification of a bacterium. J Evol Biol. 2021 Feb;34(2):246–55.

16. Yamamichi M, Letten AD, Schreiber SJ. Eco-evolutionary maintenance of diversity in fluctuating environments. Ecol Lett. 2023 Sep;26 Suppl 1:S152–67.

17. Cairns J, Borse F, Mononen T, Hiltunen T, Mustonen V. Strong selective environments determine evolutionary outcome in time-dependent fitness seascapes. Evol Lett. 2022 Jun 1;6(3):266–79.

18. Uiterwaal SF, Lagerstrom IT, Luhring TM, Salsbery ME, DeLong JP. Trade-offs between morphology and thermal niches mediate adaptation in response to competing selective pressures. Ecology and Evolution. 2020;10(3):1368–77.

19. Barbosa M, Pestana J, Soares AMVM. Predation Life History Responses to Increased Temperature Variability. PLoS One. 2014 Sep 24;9(9):e107971.

20. D. Vinebrooke R, L. Cottingham K, Norberg J Marten Scheffer, I. Dodson S, C. Maberly S, Sommer U. Impacts of multiple stressors on biodiversity and ecosystem functioning: the role of species co-tolerance. Oikos. 2004;104(3):451–7.

21. Halpern BS, Walbridge S, Selkoe KA, Kappel CV, Micheli F, D'Agrosa C, et al. A Global Map of Human Impact on Marine Ecosystems. Science. 2008 Feb 15;319(5865):948–52.

22. Bellard C, Bertelsmeier C, Leadley P, Thuiller W, Courchamp F. Impacts of climate change on the future of biodiversity. Ecology Letters. 2012;15(4):365–77.

23. Nguyen PL, Gokhale CS. On multiple infections by parasites with complex life cycles. Oikos. 2025;2025(4):e10493.

24. Silva LM, King KC, Koella JC. Dissecting transmission to understand parasite evolution. PLoS Pathog. 2025 Mar 25;21(3):e1012964.

25. Oakley MS, Gerald N, McCutchan TF, Aravind L, Kumar S. Clinical and molecular aspects of malaria fever. Trends in Parasitology. 2011 Oct 1;27(10):442–9.

26. Carlson CJ, Burgio KR, Dougherty ER, Phillips AJ, Bueno VM, Clements CF, et al. Parasite biodiversity faces extinction and redistribution in a changing climate. Science Advances. 2017 Sep 6;3(9):e1602422.

27. Buckingham LJ, Ashby B. Coevolutionary theory of hosts and parasites. j evol Biol. 2022 Feb 1;35(2):205–24.

28. Pedersen AB, Fenton A. Emphasizing the ecology in parasite community ecology. Trends in Ecology & Evolution. 2007 Mar 1;22(3):133–9.

29. Hasik AZ, King KC, Hawlena H. Interspecific host competition and parasite virulence evolution. Biology Letters. 2023 May 3;19(5):20220553.

30. Limberger R, Fussmann GF. Adaptation and competition in deteriorating environments. Proceedings of the Royal Society B: Biological Sciences. 2021 Mar 10;288(1946):20202967.

31. Greenrod ST, Cazares D, Slesak WA, Hector T, MacLean RC, King KC. Evolutionary rescue accelerates competitive exclusion in a parasite community [Internet]. bioRxiv; 2025 [cited 2025 Sep 28]. p. 2025.09.25.678511. Available from: https://www.biorxiv.org/content/10.1101/2025.09.25.678511v1

32. Greenrod STE, Cazares D, Johnson S, Hector TE, Stevens EJ, MacLean RC, et al. Warming alters life-history traits and competition in a phage community. Applied and Environmental Microbiology. 2024 Apr 16;0(0):e00286-24.

33. Kropinski AM, Mazzocco A, Waddell TE, Lingohr E, Johnson RP. Enumeration of Bacteriophages by Double Agar Overlay Plaque Assay. In: Clokie MRJ, Kropinski AM, editors. Bacteriophages: Methods and Protocols, Volume 1: Isolation, Characterization, and Interactions [Internet]. Totowa, NJ: Humana Press; 2009 [cited 2023 Jun 2]. p. 69–76. (Methods in Molecular Biology™). Available from: https://doi.org/10.1007/978-1-60327-164-6_7

34. Langmead B, Salzberg SL. Fast gapped-read alignment with Bowtie 2. Nat Methods. 2012 Apr;9(4):357–9.

35. Deatherage DE, Barrick JE. Identification of mutations in laboratory evolved microbes from next-generation sequencing data using breseq. Methods Mol Biol. 2014;1151:165–88.

36. Seemann T. Prokka: rapid prokaryotic genome annotation. Bioinformatics. 2014 Jul 15;30(14):2068–9.

37. Wick RR, Howden BP, Stinear TP. Autocycler: long-read consensus assembly for bacterial genomes [Internet]. bioRxiv; 2025 [cited 2025 Jul 29]. p. 2025.05.12.653612. Available from: https://www.biorxiv.org/content/10.1101/2025.05.12.653612v1

38. Wick RR, Holt KE. Polypolish: Short-read polishing of long-read bacterial genome assemblies. PLOS Computational Biology. 2022 Jan 24;18(1):e1009802.

39. Bouras G, Grigson SR, Papudeshi B, Mallawaarachchi V, Roach MJ. Dnaapler: A tool to reorient circular microbial genomes. Journal of Open Source Software. 2024 Jan 11;9(93):5968.

40. Li H. Minimap2: pairwise alignment for nucleotide sequences. Bioinformatics. 2018 Sep 15;34(18):3094–100.

41. RStudio Team. RStudio: Integrated Development for R. [Internet]. RStudio, PBC, Boston, M; 2020. Available from: http://www.rstudio.com/

42. R Core Team. R: A language and environment for statistical computing. [Internet]. Foundation for Statistical Computing, Vienna, Austria.; 2021. Available from: https://www.R-project.org/

43. Wickham H, Averick M, Bryan J, Chang W, McGowan LD, François R, et al. Welcome to the Tidyverse. Journal of Open Source Software. 2019 Nov 21;4(43):1686.

44. Bates D, Mächler M, Bolker B, Walker S. Fitting Linear Mixed-Effects Models Using lme4. Journal of Statistical Software. 2015 Oct 7;67:1–48.

45. Yu G, Smith DK, Zhu H, Guan Y, Lam TTY. ggtree: an r package for visualization and annotation of phylogenetic trees with their covariates and other associated data. Methods in Ecology and Evolution. 2017;8(1):28–36.

46. Tabare E, Glonti T, Cochez C, Ngassam C, Pirnay JP, Amighi K, et al. A Design of Experiment Approach to Optimize Spray-Dried Powders Containing Pseudomonas aeruginosaPodoviridae and Myoviridae Bacteriophages. Viruses. 2021 Oct;13(10):1926.

47. Visher E, Boots M. The problem of mediocre generalists: population genetics and eco-evolutionary perspectives on host breadth evolution in pathogens. Proc Biol Sci. 2020 Aug 26;287(1933):20201230.

48. Remold S. Understanding specialism when the jack of all trades can be the master of all. Proceedings of the Royal Society B: Biological Sciences. 2012 Oct 24;279(1749):4861–9.

49. Ashrafi R, Bruneaux M, Sundberg LR, Pulkkinen K, Valkonen J, Ketola T. Broad thermal tolerance is negatively correlated with virulence in an opportunistic bacterial pathogen. Evolutionary Applications. 2018;11(9):1700–14.

50. Blount ZD, Lenski RE, Losos JB. Contingency and determinism in evolution: Replaying life's tape. Science. 2018 Nov 9;362(6415):eaam5979.

51. Arribas M, Kubota K, Cabanillas L, Lázaro E. Adaptation to Fluctuating Temperatures in an RNA Virus Is Driven by the Most Stringent Selective Pressure. PLOS ONE. 2014 Jun 25;9(6):e100940.

52. Barbosa M, Inocentes N, Soares AMVM, Oliveira M. Synergy effects of fluoxetine and variability in temperature lead to proportionally greater fitness costs in Daphnia: A multigenerational test. Aquatic Toxicology. 2017 Dec 1;193:268–75.

53. Cvijović I, Good BH, Jerison ER, Desai MM. Fate of a mutation in a fluctuating environment. Proc Natl Acad Sci U S A. 2015 Sep 8;112(36):E5021–8.

54. Jaureguiberry P, Titeux N, Wiemers M, Bowler DE, Coscieme L, Golden AS, et al. The direct drivers of recent global anthropogenic biodiversity loss. Science Advances. 2022 Nov 9;8(45):eabm9982.

Extended data

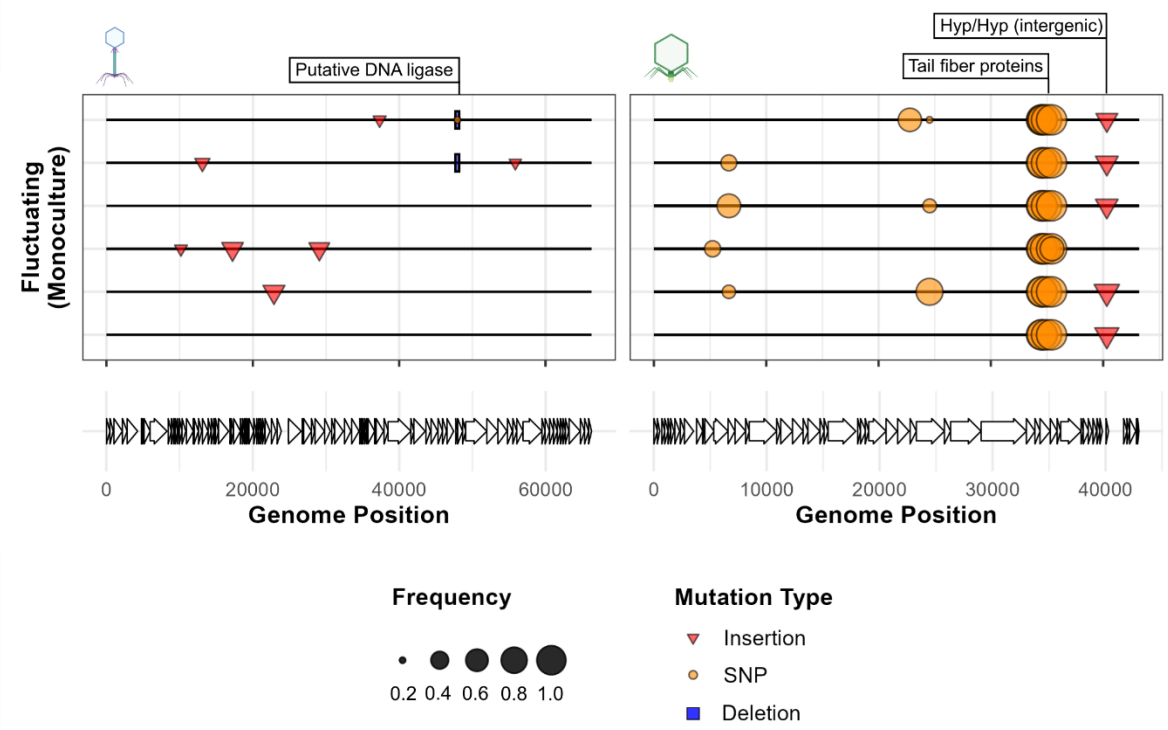

Figure S1. Fluctuating temperatures select for specialist mutations. Mutation plots show genetic variants associated with fluctuating temperatures in monoculture in phage lines. Lines represent individual biological replicates. Symbols within plots show variants across the phage genome at > 20% prevalence and which were not observed in the ancestral population. Length of deletion bars represent the size of deletion except for the ϕ14-1 deletion at ~48kb which is a 1bp deletion but given a fixed size for visibility. Labels show gene annotations for mutations found in 37°C and 42°C evolved populations [31]. Putative DNA ligase in ϕ14-1 was originally annotated a hypothetical protein but has high homology to Pseudomonas phage PhL_UNISO_PA-DSM_ph0031 DNA ligase protein.

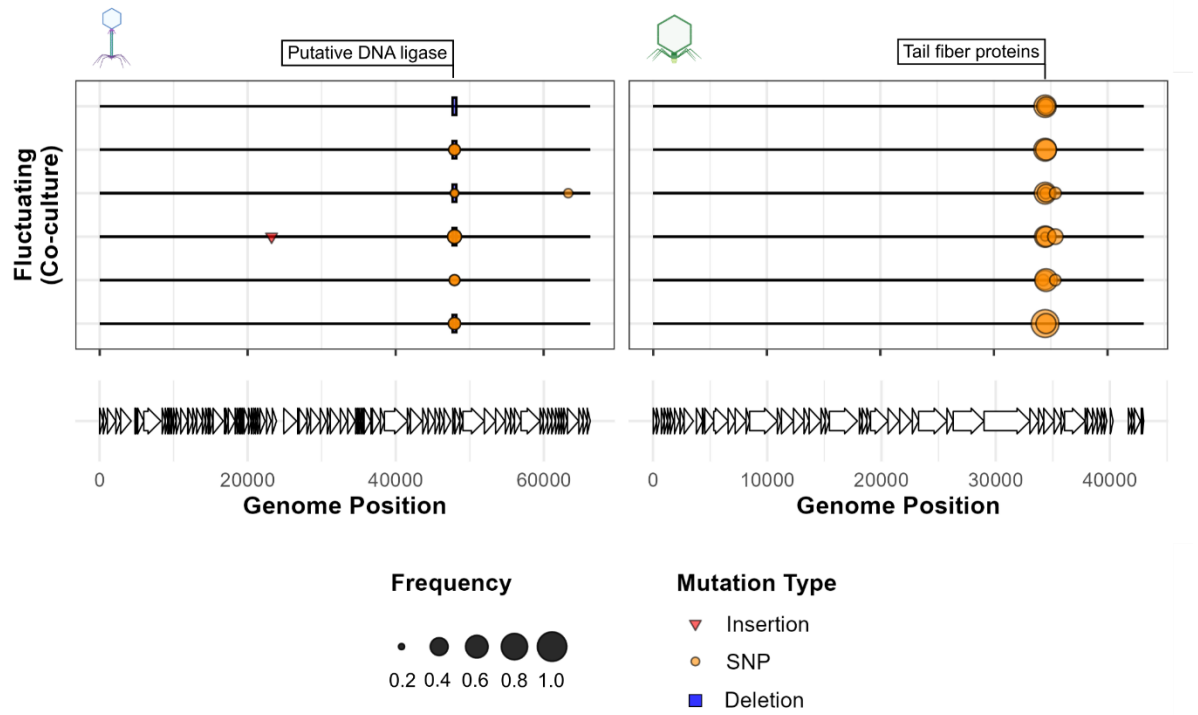

551

552 **Figure S2. Competition restricts the acquisition of high frequency mutations.** Mutation plots show
553 genetic variants associated with fluctuating temperatures in co-culture in phage lines. Lines represent
554 individual biological replicates. Symbols within plots show variants across the phage genome at > 20%
555 prevalence and which were not observed in the ancestral population. Length of deletion bars
556 represent the size of deletion except for the ϕ14-1 deletion at ~48kb which is a 1bp deletion but given
557 a fixed size for visibility. Labels show gene annotations for mutations found in 37°C and 42°C evolved
558 populations [31]. Putative DNA ligase in ϕ14-1 was originally annotated a hypothetical protein but has
559 high homology to Pseudomonas phage PhL_UNISO_PA-DSM_ph0031 DNA ligase protein.

560